

Open Access Article

## DESIGN AND ANALYSIS OF PROTEIN SEPARATION TECHNIQUE IN A MICROFLUIDIC DEVICE

**Raghunathareddy M V**

Dept of ECE, Cambridge Institute of Technology, Bangalore-36  
Email: hod.ece@cambridge.edu.in

**Indumathi G**

Dept of ECE, Cambridge Institute of Technology, Bangalore-36

### Abstract

Electrophoretic transport across channel stream has been analyzed with different pH concentration of protein molecules. Isoelectric focusing chip model with separating laminar flow region has been introduced in the designed channel. This laminar stream separated the protein molecules with different concentration. Four different protein molecules with different isoelectric point values are considered in the analysis. Protein 1, Protein 2, Protein 3 and Protein 4 has been analyzed for different pressure distribution and velocity magnitude. Maxim pressure distribution of  $1296.5 \times 10^{-5} \text{Pa}$  is observed and velocity magnitude of  $20 \times 10^{-5} \text{m/s}$  is obtained for designed channel.

**Keywords:** Isoelectric, Microfluidic, Channel, Protein, pH Concentration, laminar flow

### 抽象的

已经用蛋白质分子的不同 pH 浓度分析了跨通道流的电泳传输。在设计通道中引入了具有分离层流区域的等电聚焦芯片模型。这种层流分离了不同浓度的蛋白质分子。在分析中考虑了具有不同等电点值的四种不同蛋白质分子。蛋白质 1、蛋白质 2、蛋白质 3 和蛋白质 4 已针对不同的压力分布和速度大小进行了分析。观测到的最大压力分布为  $1296.5 \times 10^{-5} \text{Pa}$ ，获得的设计通道速度为  $20 \times 10^{-5} \text{m/s}$ 。

**关键词:** 等电、微流体、通道、蛋白质、pH 浓度、层流

### Introduction

Authors Laurence and Piero et.al studied interaction between DNA proteins with microfluidic channels analyzed the laminar flow of molecules. Optically trapped and mechanical isolated molecules have been investigated with microfluidic channel system. Construction techniques and material to be considered for future fabrication has been discussed [1]. In another context authors worked on gradient free determination of isoelectric points of protein

chips. Gradient change due to pH value. Seven types of proteins are classified with the help of designed microfluidic channels [2]. In another work capillary gel electrolysis and capillary isoelectric focusing has been carried out in microfluidic channel design. Benchtop microfluidic chamber has been designed for flow of bio sample in the microfluidic channel designed. Designed aimed at controlling the uniform velocity [3]. Microfluidic mixers are considered in microfluidic channel for proper

mixing of biomolecule's introduced for detection of protein [4]. Authors analyzed the food flow with the microfluidic channel. In concern with safety, food industry is coming with the microfluidic channel for separation of contamination with the sensitive designs [5]. Microfluidic platforms have been considered for studying cell culture system. Computational fluid dynamic has been implemented to simulate the microfluidic channel. Fluid flow process and velocity distributions, pressure distributions throughout the microfluidic channel have been evaluated [6]. Particle suspension has been identified and considered for fluid flow analysis. Different types of microfluidic channel have been used to analyze the flow separation between. A level set method has been considered for design of microfluidic channel and computational fluid dynamic. Droplet size in focusing shape micro channel has been considered. Formation of droplet and varying size of output port has been investigated [7]. Parallel microchannel has been used for simulation of fluid flow and micro channel. Generalized transport equations are incorporated in the software simulation. Pressure, temperature and velocity distribution on the channels are analyzed. Aspect ratio increases with increasing Reynolds number and decrease with outlet thermal resistance value [8]. Lab on chip system is developed for lysis of mammalian cells which is essential part of different lab on chip application methods. Computational fluid dynamic method has been used for analyzing the micro molecules flow in microfluidic channel. In other context authors designed microfluidic chip for measuring the pH gradient. It consists of inlet reservoirs and output reservoir and reservoir which holds bio sample. Acid is flowing through the reservoir with mixing channel. pH value is

denoted by universal indicator [9]. Droplet formation is popular microfluidic application precise control over flow and associated suspension. Force exerted by neutral dielectric object in presence spatially non uniform dielectric field is defined as dielectrophoretic. In this work author proposed the how optical tweezers can be used to quantify the dielectrophoretic force experienced by red blood cells of human [10]. Curved duct microfluidic channel has been investigated for flow of micro molecules. Geometrical optimization of sensing channel has been calculated. Experimental and computational analysis of microfluidic channel is carried out for velocity distribution, pressure distribution and flow rate monitoring in working process [11]. Droplet formation with microfluidic T junction has been investigated with varying geometrical optimizations. Effect of wettability of channels due to formation of droplet is analyzed. Effect of contact angle reduction and flow rate dispersion has been verified. Significant droplet size variation mechanism has been tested.

#### **Design and Working Principle:**

In this work, Electrophoretic Transport and the Laminar Flow is used separate protein in the stream. Four different proteins are considered and are separated with the application of electric field. Proteins are the macromolecules which can be separated with the electrophoresis process. With the pH and electric potential, the macromolecules are made to flow in the desired directions. The pH at which net charge of the particle is zero is called iso-electric point. A positive molecule will move along the direction of the field whereas negative molecule will move in opposite direction. The model has following dimensions as shown in figure. Width of total channel designed is 0.0035m. Height of electrode

is 0.03m. Isoelectric point of protein 1 is 4.7, protein 2 is 6.1, protein 3 is 7.5, protein 4 is 9. Protein diffusivity of  $5E-10$  m<sup>2</sup>/s, Average carrier fluid velocity  $1.5E-4$  m/s, Inlet protein concentration of 1 mol/m<sup>3</sup>, Voltage 0.15 V, Weak acid inlet concentration of 100 mol/m<sup>3</sup>,

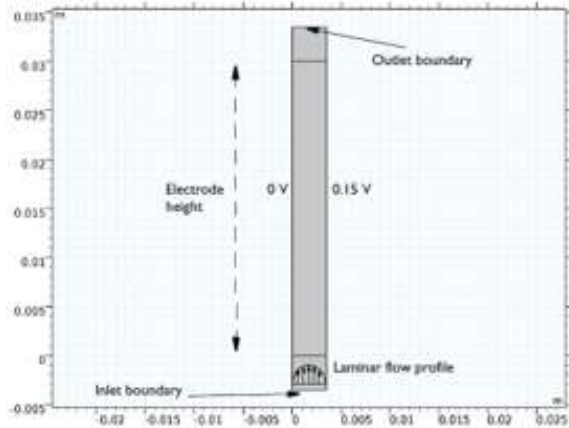


**Figure 1:** Channel design in with boundary conditions

Electrophoretic transport ionic species with the process of convection, migration and diffusion in the presence of electric field inside the microfluidic channel. A physics-controlled mesh is as shown in the figure which is finer. Figure 1 and Figure 2 shows the dimensions of

Weak base inlet concentration of 100 mol/m<sup>3</sup>, pKa of weak acid is 8, pKa of weak base is 6 and Weak acid mobility of  $2.4E-13$  s·mol/kg and mobility of weak base will be  $2.5E-13$  s·mol/kg.

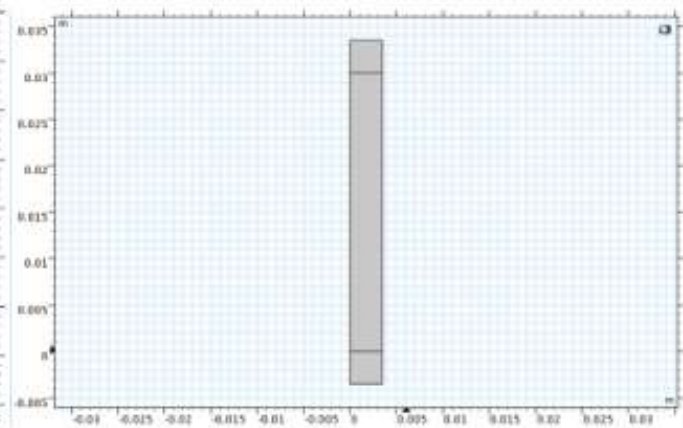


**Figure 2:** Channel design in COMSOL

microfluidic channel for isoelectric protein separation. Possible laminar profile available in the inlet boundary condition is showing figure 1. Major boundary condition assigned the structure is inlet and outlet for flow of fluid introduced.

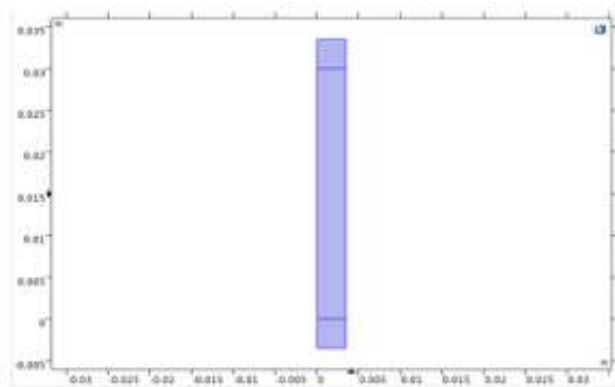


**Figure 3:** Microchannel design in COMSOL

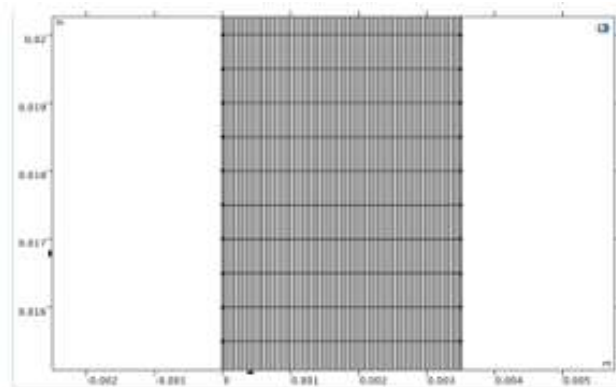


**Figure 4:** FEA model of microchannel

Figure 3 and Figure 4 shows the FEA model to simulate the channel environment in COMSOL Multiphysics. Channel is discretized with the

controlled mesh environment. Number of mesh element obtained during the meshing process are 1,23,323.

## Results and Discussion:

### Velocity Distribution

Velocity distribution of the fluid is as shown below. We can observe high velocity in the center region and reduces near boundary of the channel. Figure 5 and Figure 6 shows the velocity and contour pressure distribution in the

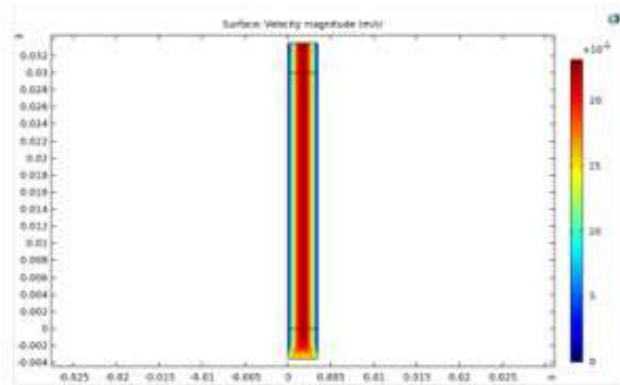


Figure 5: Velocity magnitude of channel

channel designed. Maximum velocity magnitude of  $20 \times 10^{-5}$  is achieved at the center portion of microfluidic channel. Minimum velocity magnitude of  $0.5 \text{ m/s}$  is obtained as shown in Figure 5. Red color in the figure indicates the maximum pressure at the center position of microchannel.

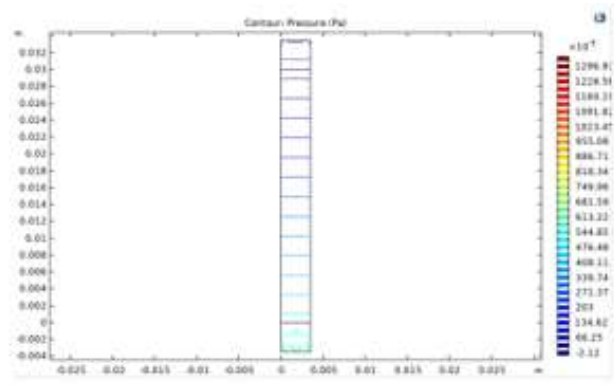
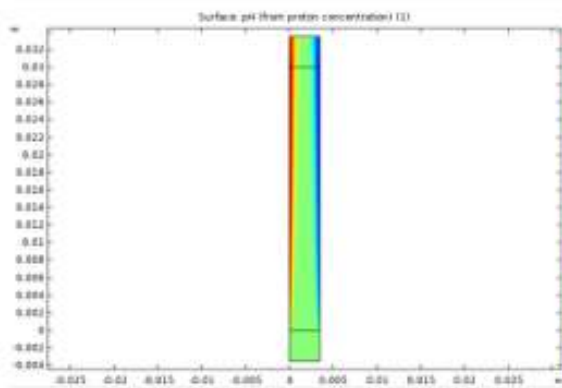


Figure 6: Contour pressure of channel

### Pressure Distribution

At the inlet it has high pressure and reduces as it flows towards outlet. pH distribution the cells is as shown in the figure. Higher pH at left boundary and lower pH at right boundary. Conductivity of the electrolyte is minimum at the boundary. A very high conductivity at the inlet and middle region of the channel. Electrolyte conductivity was maximum at the inlet and

gradually decreases at the outlet region. Maximum conductivity of  $0.4 \text{ s/m}$  is achieved at the inlet portion of channel concentration slightly maximum at the left boundary and minimum at the right boundary. pH concentration at medium range at inlet region. Figure 7 and Figure 8 shows the pH value and surface electrolyte conductivity.



**Figure 7:** pH value from protein concentration 1

The applied potential the left boundary is 0 volts and right boundary 0.15 volts. The potential distribution diagram shows high potential at the

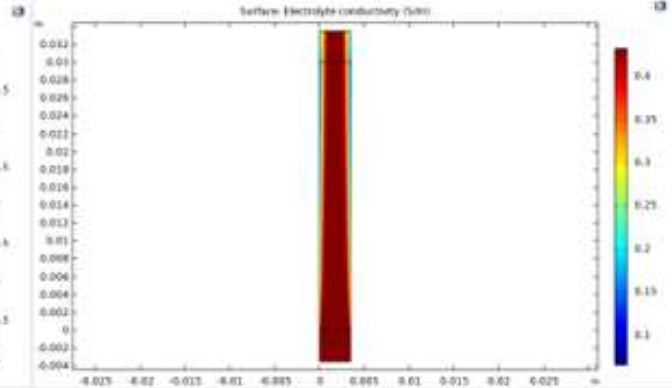


**Figure 8:** Surface electrolyte conductivity in channel

right and low potential at the left boundary of the channel.

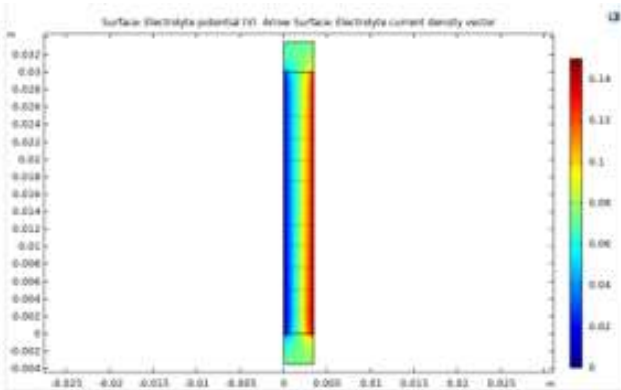


**Figure 9 :** Electrolyte current density vector for channel

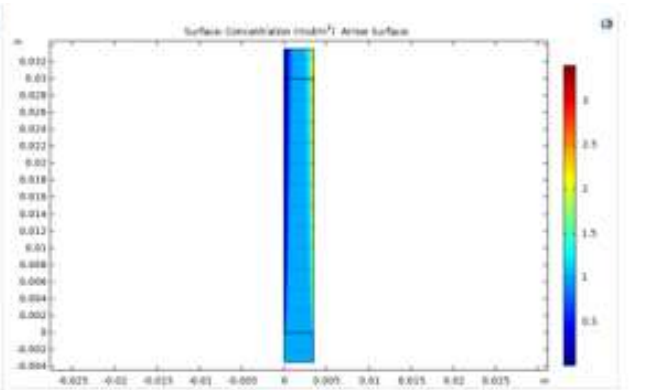


**Figure 10:** Arrow surface concentration of channel protein 1

**Protein - 1 Molar Concentration**

The molar concentration of the protein 1 is shown below. It has an iso-electric point of 4.7. Protein 1 is concentrated at the right boundary of the channel.

**Protein - 2 Molar Concentration**

The molar concentration of the protein 2 is shown below. It has an iso-electric point of 6.1. Protein 2 is concentrated somewhere between the center and towards right side region

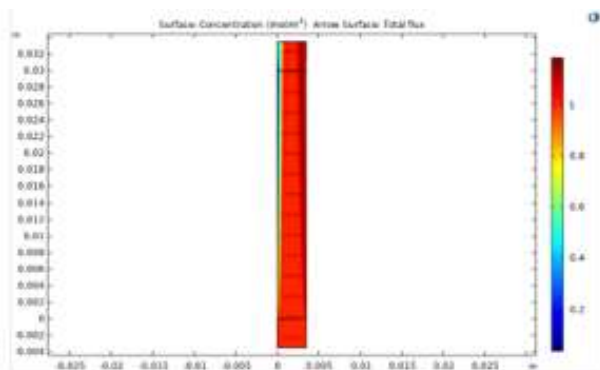


Figure 11: Total Flux of channel protein 2

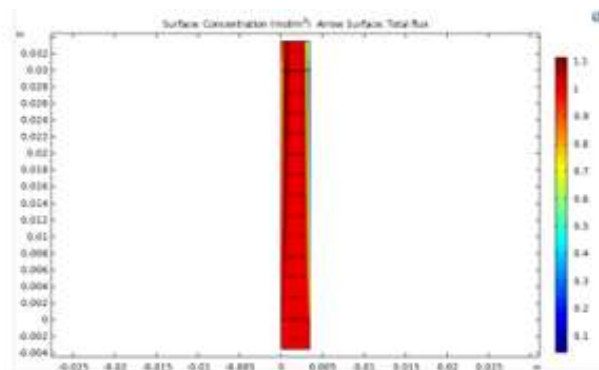


Figure 12: Total Flux of channel in arrow surface for protein 3

### Protein - 3 Molar Concentration

The molar concentration of the protein 3 is shown below. It has an iso-electric point of 7.5. Protein 3 is concentrated somewhere between the center and towards left side region.

### Protein - 4 Molar Concentration

The molar concentration of the protein 4 is shown below. It has an iso-electric point of 9. Protein 4 is concentrated at the left boundary of the channel.

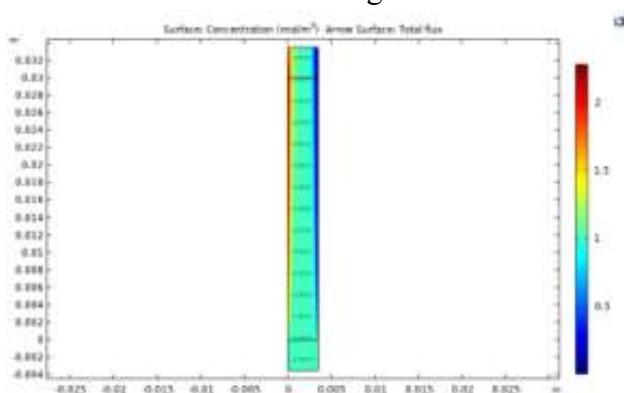


Figure 13: Surface concentration of protein 4

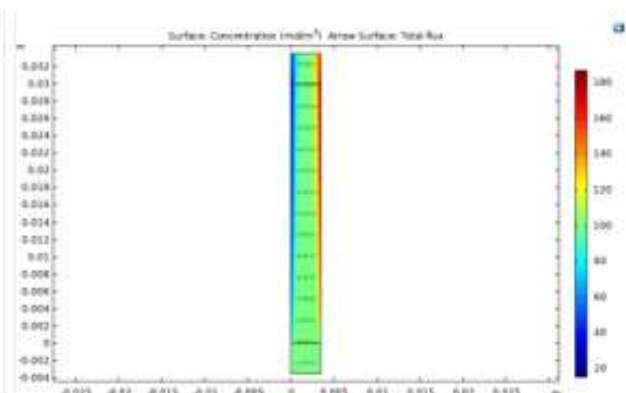


Figure 14: Weak acid molar concentration

Molar concentration of the protein 1 is maximum at the right boundary of the channel and least at the left boundary of the channel. Protein 2 has shown total flux is maximum at the right boundary and less at the left boundary of channel.

### Weak acid Molar Concentration

The weak acid has an average negative charge and are transported along with the right boundary of the channel

### Weak base Molar Concentration

The weak base has an average positive charge and are transported along with the left boundary of the channel

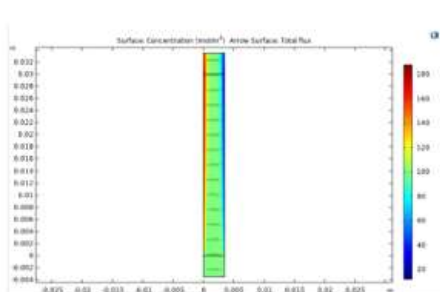


**Figure 15:** Weak base molar concentration spatial coordinate X

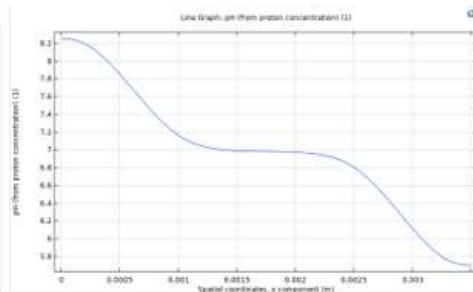


**Figure 16:** Protein concentration with

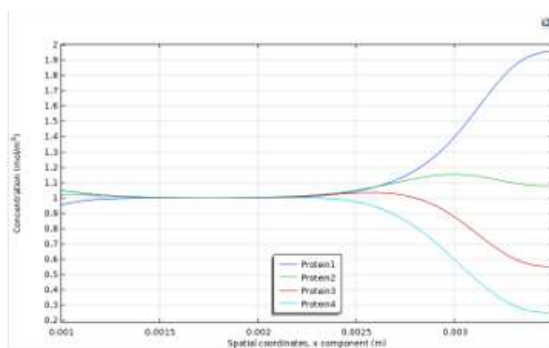
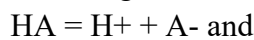


**Figure 17:** Protein concentration in X component

The figure 16 shows the pH concentration profile at the outlet region. The figure 17 shows the protein concentration at the outlet region.

### Weak Acids and pKa:

The strength of an acid can be determined by its dissociation constant,  $K_a$ . Acids that do not dissociate significantly in water are weak acids. The dissociation of an acid is expressed by the following reaction:



the dissociation constant  $K_a = \frac{[H^+][A^-]}{[HA]}$

When  $K_a < 1$ ,  $[HA] > [H^+][A^-]$  and HA is not significantly dissociated. Thus, HA is a weak acid when  $k_a < 1$ . The lesser the value of  $K_a$ , the weaker the acid. Similar to pH, the value of  $K_a$  can also be represented as pKa.

$$pK_a = -\log K_a.$$

The larger the pKa, the weaker the acid. pKa is a constant for each conjugate acid and its

conjugate base pair. Most biological compounds are weak acids or weak bases.

### ***The Henderson-Hasselbalch equation:***

Dissociation of a weak acid is mathematically described by the Henderson-Hasselbalch equation

$$K_a = \frac{[H^+][A^-]}{[HA]} \text{ or}$$

$$K_a = [H^+] \times \frac{[A^-]}{[HA]}$$

$$\log K_a = \log [H^+] + \log \left\{ \frac{[A^-]}{[HA]} \right\}$$

$$-\log [H^+] = -\log K_a + \log \left\{ \frac{[A^-]}{[HA]} \right\}$$

$$pH = pK_a + \log \left\{ \frac{[A^-]}{[HA]} \right\}$$

So, if CB = conjugate base and WA = weak acid, then:

$$pH = pK_a + \log \left\{ \frac{[CB]}{[WA]} \right\}$$

$$\text{Note: } pH = pK_a \text{ when } [CB] = [WA]$$

### **The pH scale**

An acidic solution is one in which  $[H^+] > [OH^-]$

In an acidic solution,

$$[H^+] > 10^{-7}, pH < 7.$$

A basic solution is when

$$[OH^-] > [H^+].$$

In a basic solution,

$[\text{OH}^-] > 10^{-7}$ ,

$\text{pOH} < 7$ , and  $\text{pH} > 7$ .

When the  $\text{pH} = 7$ , the solution is neutral. Physiological pH range is 6.5 to 8.0. Figure 10 to 17 shows the molar concentration of protein 1 to protein 4. Molar concentration has shown high variation from left to right or right to left boundary. Based on variation with isoelectric point value there is change in molar concentration of protein 1, protein 2 and protein 3 and protein 4. Weak acid and weak base have also shown changes with molar concentration in the channel designed. Variation in concentration from inlet to outlet is shown in Figure 17. It is observed that molecules with net charge of positive travel in the direction of electric field and negative net charges travel in the opposite direction of positive charge. It is found that channel has more pressure at the inlet and less pressure at the outlet. Velocity magnitude at outlet is more than the inlet region of channel.

### Conclusion

In the proposed work isoelectric separation model has been constructed for free flow electrophoretic devices with interfaces such as laminar flow and electrophoretic transport. Four different types of protein with different pH concentration have been considered in analysis. Electric field is introduced in the microfluidic channel designed. Macromolecules with different pH concentration is made flow through the channel by electrophoresis. Channels are analyzed for different velocity and pressure distribution with varying input and output flow rate. Maximum pressure distribution of  $1296.5 \times 10^{-5} \text{Pa}$  has been observed in micro channel designed. Maximum velocity magnitude of  $20 \times 10^{-5} \text{m/s}$  is obtained.

### Acknowledgement

Author would like the all researchers and staff of Cambridge institute of technology for providing the necessary support for carrying out the effective research and helping to complete the manuscript successfully.

### References:

1. Brewer, L., Bianco, P. Laminar flow cells for single-molecule studies of DNA-protein interactions. *Nat Methods* 5, 517–525 (2008). <https://doi.org/10.1038/nmeth.1217>
2. Łapińska, Urszula et al. "Gradient-free determination of isoelectric points of proteins on chip." *Physical chemistry chemical physics : PCCP* 19 34 (2017): 23060-23067.
3. Wan Shi Low, Nahrizul Adib Kadri, Wan Abu Bakar bin Wan Abas, "Computational Fluid Dynamics Modelling of Microfluidic Channel for Dielectrophoretic BioMEMS Application", *The Scientific World Journal*, vol. 2014, Article ID 961301, 11 pages, 2014. <https://doi.org/10.1155/2014/961301>.
4. Inguva V, Kathuria SV, Bilsel O, Perot BJ. Computer design of microfluidic mixers for protein/RNA folding studies. *PLoS One*. 2018;13(6):e0198534. Published 2018 Jun 20. doi:10.1371/journal.pone.0198534.
5. Xie, Z, Pu, H, Sun, D-W. Computer simulation of submicron fluid flows in microfluidic chips and their applications in food analysis. *Compr Rev Food Sci Food Saf*. 2021; 20:3818–3837.

- <https://doi.org/10.1111/1541-4337.12766>.
6. Christine Poon, Measuring the density and viscosity of culture media for optimized computational fluid dynamics analysis of in vitro devices, 2020, doi: <https://doi.org/10.1101/2020.08.25.266221>
  7. Xiangdong Xue, Mayur K. Patel, Maiwenn Kersaudy-Kerhoas, Marc P.Y. Desmulliez, Chris Bailey, David Topham, Analysis of fluid separation in microfluidic T-channels, *Applied Mathematical Modelling*, Volume 36, Issue 2, 2012, Pages 743-755, ISSN 0307-904X, <https://doi.org/10.1016/j.apm.2011.07.009>.
  8. Shivaji Rao Devakathe , Rajesh S. , Satish Kumar G., 2019, CFD Simulation of Fluid Flow and Heat Transfer in Micro Channels, *International journal of engineering research & technology (ijert)*, Volume 08, Issue 07 (July 2019).
  9. Zhao, Y.C., Vatankhah, P., Goh, T. et al. Hemodynamic analysis for stenosis microfluidic model of thrombosis with refined computational fluid dynamics simulation. *Sci Rep* 11, 6875 (2021). <https://doi.org/10.1038/s41598-021-86310-2>.
  10. Mehrzad Sasanpour, Ali Azadbakht, Parisa Mollaei, and S. Nader S. Reihani, "Proper measurement of pure dielectrophoresis force acting on a RBC using optical tweezers," *Biomed. Opt. Express* 10, 5639-5649 (2019), <https://doi.org/10.1364/BOE.10.005639>.
  11. Bharat Kalsi ,Vinay Aggarwal, Satbir Singh Sehgal, Experimental and Computational Fluid Dynamic Analysis of Mixing Problems in Microfluidic Device, *Indian Journal of Science and Technology*, DOI: 10.17485/ijst/2016/v9i36/101407.
  12. Chen, N., Wu, J., Jiang, H., & Dong, L. (2012). CFD Simulation of Droplet Formation in a Wide-Type Microfluidic T-Junction. *Journal of Dispersion Science and Technology*, 33, 1635 - 1641.
  13. Sathyanarayanan, G., Haapala, M., Dixon, C., Wheeler, A. R., Sikanen, T. M., A Digital-to-Channel Microfluidic Interface via Inkjet Printing of Silver and UV Curing of Thiol-Enes. *Adv. Mater. Technol.* 2020, 5, 2000451. <https://doi.org/10.1002/admt.202000451>
  14. Zhang, Y., Chen, X. Dielectrophoretic microfluidic device for separation of red blood cells and platelets: a model-based study. *J Braz. Soc. Mech. Sci. Eng.* 42, 89 (2020). <https://doi.org/10.1007/s40430-020-2169-x>
  15. Zhang, Y., Chen, X. Blood cells separation microfluidic chip based on dielectrophoretic force. *J Braz. Soc. Mech. Sci. Eng.* 42, 206 (2020). <https://doi.org/10.1007/s40430-020-02284-8>